IAC-12.A6.1.16

OBSERVATIONS STRATEGIES FOR SPACE DEBIS ON HIGHLY-ECCENTRIC MEO ORBITS

Andreas Hinze
Astronomical Institute, University of Bern, Switzerland, andreas.hinze@aiub.unibe.ch

T. Schildknecht
Astronomical Institute, University of Bern, Switzerland, thomas.schildknecht@aiub.unibe.ch
A. Vananti
Astronomical Institute, University of Bern Switzerland, alessandro.vananti@aiub.unibe.ch
H. Krag
ESA/ESOC, Germany, holger.krag@esa.int
T. Flohrer
ESA/ESOC, Germany, tim.flohrer@esa.int

The Medium Earth Orbit region (MEO) becomes increasingly populated as new satellite constellations are deployed or existing constellations are replenished with new satellites. Therefore we could also expect an increasing amount of space debris including small size objects in this region. After the already investigated circular MEO orbits of the GPS and GLONASS constellations the Astronomical Institute of the University of Bern (AIUB) developed survey and follow-up strategies for the search of space debris in highly-eccentric orbits in the MEO region. None of these orbital planes have been investigated systematically for potential space debris so far. In this paper we present different survey and follow-up strategies for searching space debris objects in highly-eccentric orbits and to acquire orbits which are sufficiently accurate for cataloguing with the objective of maintaining orbits over longer time spans. Simulations for survey and follow-up observations were performed to compare the performance of different strategies.

I. INTRODUCTION

The largest part of the mass launched into space actually becomes ‘space debris’ or ‘orbital debris’ immediately after launch. After the accomplished mission, even the payload will become space debris eventually. The increasing number of space debris creates an increasing risk for space missions. In higher regions, where no “natural” clean-up effects exist, the only way of dealing with the space debris threat is the continuous observation of the space debris environment. While the Low Earth Orbit (LEO) has been studied extensively during the last decades and the geostationary ring (GEO) [RD 01, RD 02] and the geostationary transfer orbit (GTO) [RD 03] have been continuously observed during the last years the next step is the extension of the ongoing space debris surveys to new orbital regions, in particular to the increasingly populated Medium Earth Orbit region (MEO). The space debris environment in the MEO region has not been systematically investigated so far and is thus largely unknown.

II. TLE POPULATION

The selected subset of the MEO region includes objects within the following limits:

$$60\text{deg} < i < 67\text{deg}$$

$$0.5 < e < 0.8$$

$$20000\text{km} < a < 30000\text{km}$$

A semi major axis between 20000km and 30000km corresponds to a mean motion of about 2 revolutions per day. We set no limit in right ascension of the ascending node (RAAN) and for the perigee. Finally 171 objects were selected using the USSTRATCOM catalogue of unclassified objects (January 2012). This selected population (TLE population) includes MOLNIYA satellites, MERIDIAN satellites, OKO satellites as well as some known space debris. Figure 1 shows the distributions of the orbital elements. The nodes are distributed over the whole range of right ascension with a concentration between 0deg and 200deg. The inclinations are concentrated around the nominal value of 63.4deg (critical inclination). Based on the distribution of the eccentricity it was possible to separate a subgroup consisting of 35 objects including rocket bodies (10), debris (20) and Russian Oko satellites (5) with an eccentricity of less than 0.65. These objects have similar orbital elements and launch date, therefore it is likely that these objects belong together. The relations between the orbital elements are shown in Figure 2 were objects with an eccentricity of less than 0.65 are given in green. Objects with a perigee less than 180deg and therefore with an apogee above the southern hemisphere are given in red. Simulations have been performed to analyse the evolution of the orbital elements. For this propagation, a full force model was used including the gravitational attraction of Sun and Moon. Further Earth’s potential coefficients up to terms of degree and order 12, the perturbations due to the Earth tides, the corrections due to general relativity, and a simple model for the direct radiation pressure [RD 04]. For the radiation pressure an area-to-mass

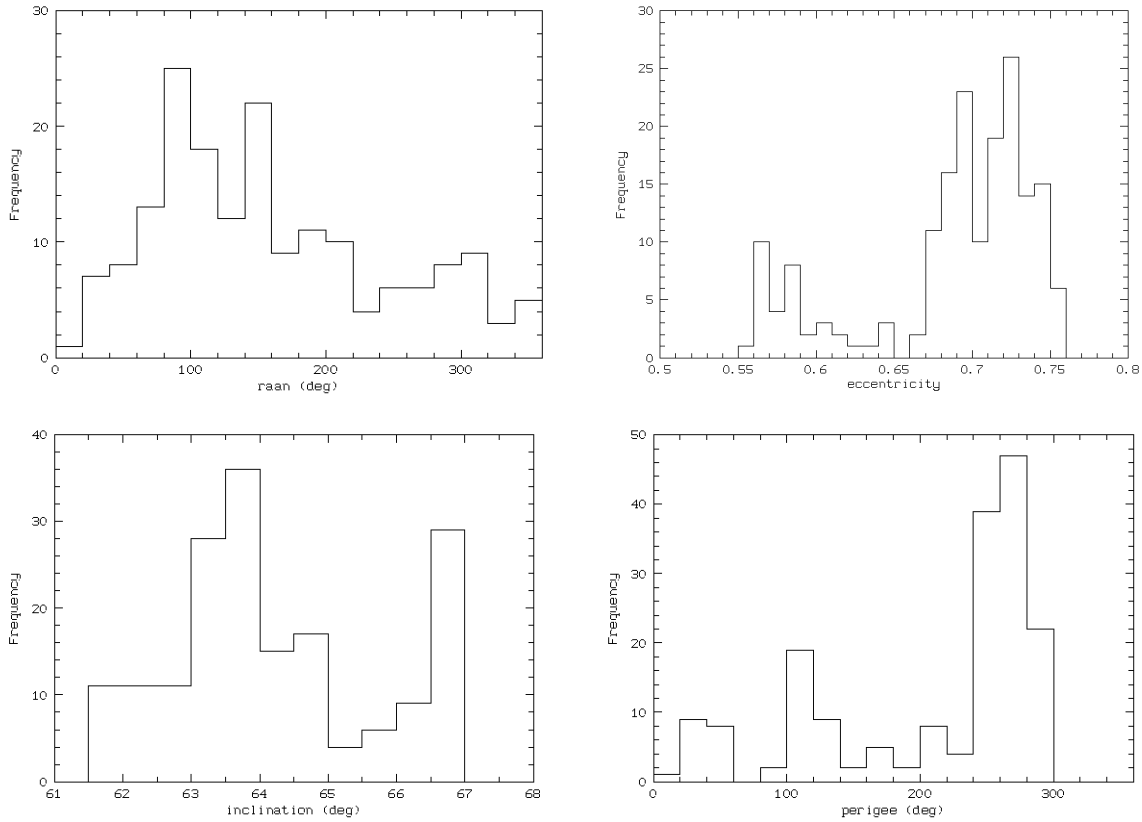

Figure 1: Distribution of four orbital elements of the analysed TLE population at epoch January 2012.

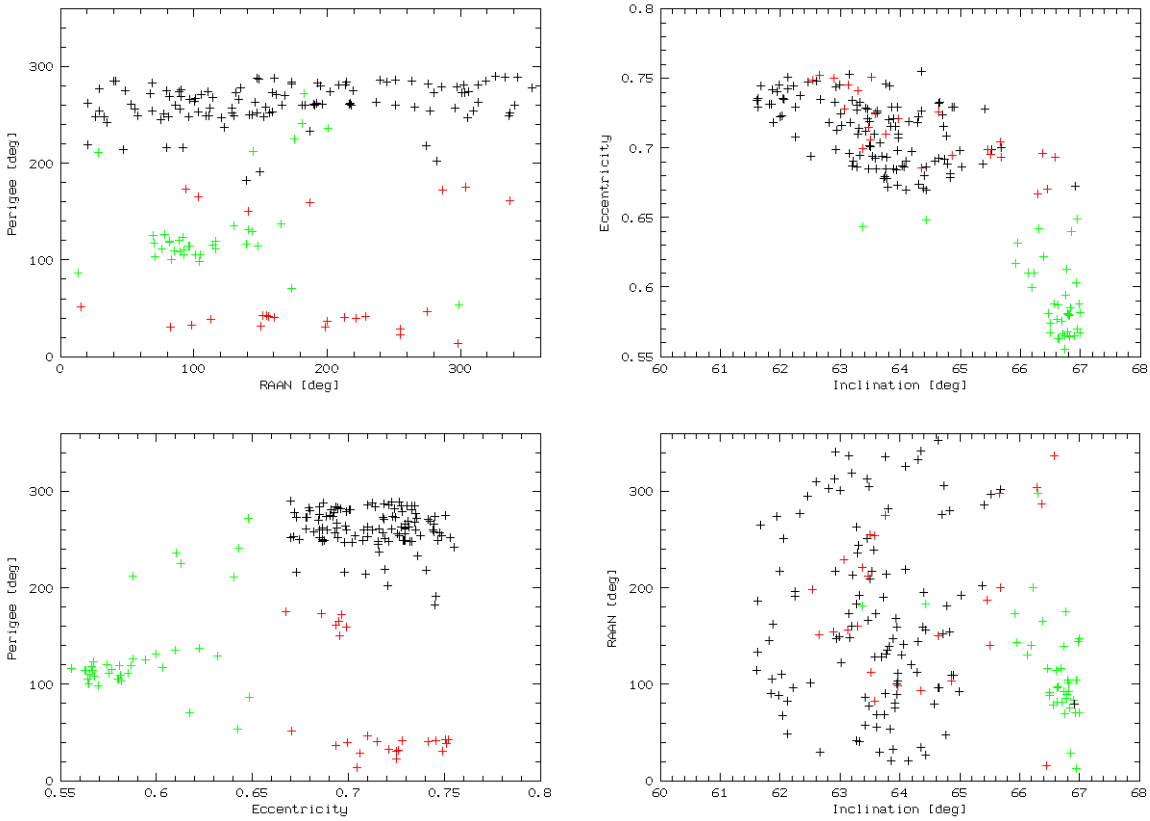

Figure 2: Relation between some orbital elements of the analysed TLE population. Green means that these objects have an eccentricity less than 0.65 and red means that these objects have a perigee less than 180deg.

ratio (AMR) value of 0.009 both, for air drag and radiation pressure, was used.

Figure 3 shows the evolution of the orbital elements over 20 years. As mentioned before, based on the distribution of the eccentricity it is possible to separate a subgroup. Therefore objects with an eccentricity of less than 0.65 are given in green. The daily drift of the nodes for the analysed TLE population is about -0.1 to -0.2deg/day which corresponds to a drift of about -35 to -70deg/year. Most of the objects keep their eccentricity over the simulated time interval whereas the inclination and the perigee changes for objects with an initial eccentricity of less than 0.65. However, there is almost the same distribution of the orbital elements after 20 years. Therefore we can expect that the current distribution represent the initial distribution.

III. SURVEY STRATEGIES

Performing optical surveys using ESA's Space Debris Telescope, the 1-m Zeiss telescope at the Optical Ground Station (OGS) with a Field of View (FoV) of 0.7x0.7deg^2 a short FoV crossing time can be expected. Assuming a maximum angular velocity of about 30arcsec/sec, an object crosses the FoV in about 84sec. Therefore at maximum four consecutive observations with a gap time of 20sec can be performed before the objects leave the field. If the maximum angular velocity is about 20arcsec/sec we get a maximum FoV crossing time of 126sec and seven consecutive observations would be possible. Figure 4 (left) shows the topocentric angular velocities during an observation night in the RA/DE system as a function of declination. The minimal velocity is about 7arcsec/sec for a declination between 60deg and 70deg. To cover a wide range of objects, surveys at a fixed declination stripe are preferred. At a fixed stripe at 55deg declination 84 objects of the TLE population with angular velocities of less than 15arcsec/sec would crossed the FoV within one year. Assuming objects with a mean motion of about two revolutions per day observing a single field for twelve hours during one night would be the optimum. All objects in a specified orbital plane cross the FoV within this period. During the winter season observation during twelve hours per night are possible but summer nights may be as short as 6 hours only at the ESA telescope. Nevertheless a selected field with declination of 55deg and right ascension in anti-sun direction is observable under good phase angle conditions during the whole night. The phase angle ranges between 10deg and 130deg for objects with an angular velocity of less than 30arcsec/sec (Figure 4 right).

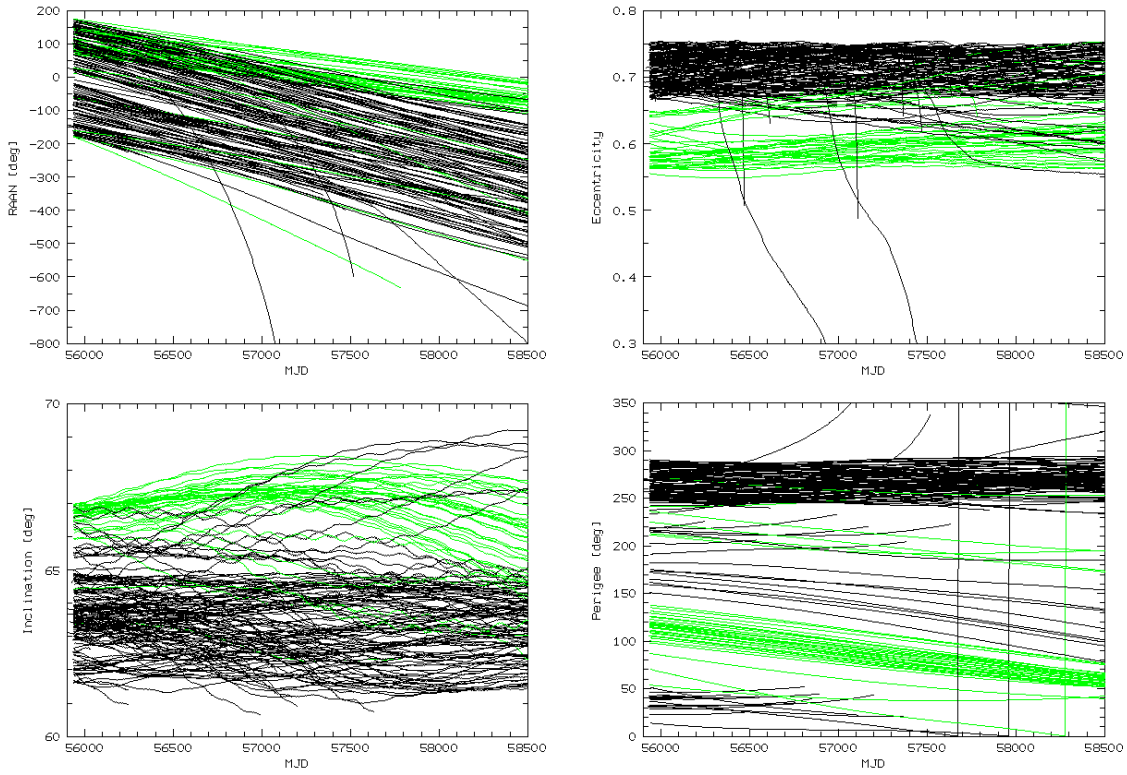

Figure 3: Evolution of the orbital elements of the selected TLE population for 20 years. Objects with an eccentricity of less than 0.65 are given in green.

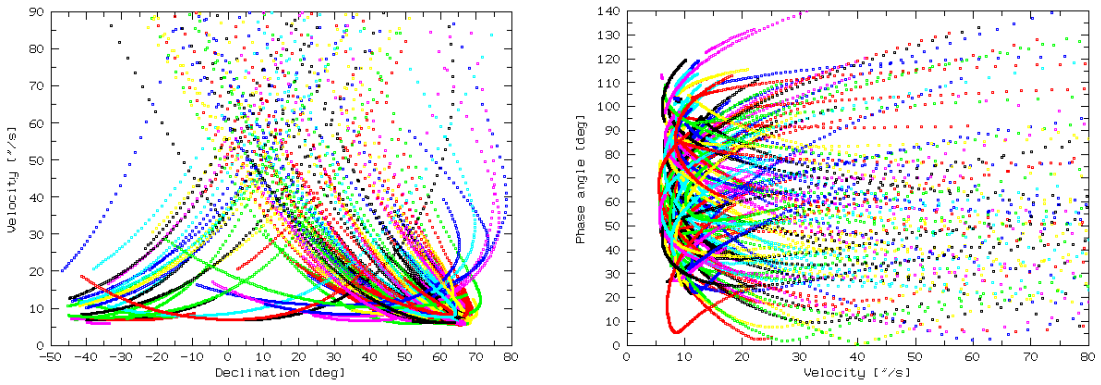

Figure 4: Topocentric angular velocities as a function of DE (left). Phase angle as a function of the angular velocity (right).

IV. FOLLOW UP STRATEGIES

Observations of one object performed during a single FoV crossing creating a so called tracklet. Using the ESA telescope, a gap time of 20sec and assuming an angular velocity of 20arcsec/sec, a tracklet may consist up to 6 consecutive observations to simulate the follow-up strategies. This is just the best case and we therefore chose a tracklet with four observations. With an arc length of about 1 minute a first orbit can be determined. But the accuracy of this orbit is of low quality and a rediscovery after one day virtually impossible. Therefore follow up observations during the night of discovery should be performed to acquire a secured orbit and to maintain orbits over longer time spans.

In order to estimate the frequency and the time of such follow-up observations, a synthetic population with 100 objects has been simulated ("true" orbit). The limits of the orbital elements were chosen according to the limits of the TLE population. A homogenous distribution of each orbital element was assumed.

The discovery tracklet consists of four observations with an arc length of one minute. A position error of σ=0.5arcsec was assumed for the accuracy of the single observation. This is a typical error for observations from the ESA telescope. Circular orbits were determined using all four observations.

An orbit was determined from the observations and propagated into the future. In order to recover an object after a few hours it is necessary that the determined orbit represents the "true" orbit accurately during this time interval. The differences between the ephemerides of the propagated orbit and the "true" ones are given by

$$\Delta = \arccos\left(\sin\delta_t \sin\delta_d + \cos\delta_t \cos\delta_d \cos\Delta\alpha\right) \quad [1] \qquad (1)$$

where δ_t and δ_d are the declination values from the "true" and the determined orbit and $\Delta\alpha$ is the difference in right ascension α [RD 04].

Figure 5 shows the differences between the determined and true orbits. For all simulated orbits the differences are smaller than 0.5deg within the first twenty minutes after the discovery. The differences have to be smaller than half of the FoV of the instrument for a successful recovery. This implies that most objects may be successfully recovered within twenty minutes after the discovery using the ESA telescope.

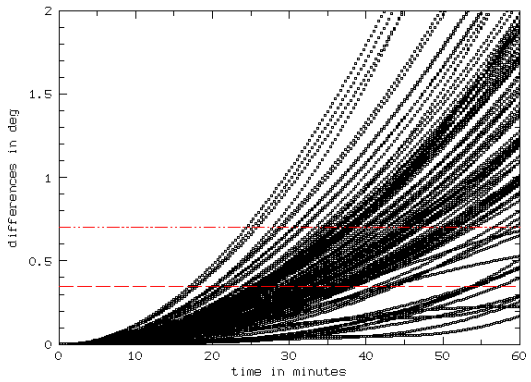

Figure 5: Difference Δ between "true" and circular orbit representing four discovery observations spanning one minute of time. Each curve represents the result from one of 100 simulated MEO orbits.

A first serie of follow-up observations was simulated 30 minutes after the discovery. Observation arcs of 30 minutes are long enough to reliably determine elliptical orbits. All observations (detection and first follow-up tracklets) were used to determine the orbits. The differences are smaller than 0.3° within 90 minutes and smaller than 2° within three hours. Therefore, a second series of follow-up observation was simulated 90 minutes after the discovery and a third one three hours after the discovery. After each follow-up observation an elliptical orbit was determined using all available observation tracklets. Figure 6 shows the differences between the final determined orbit including the detection and three follow-up observations and the true orbit. Best results are obviously obtained after a full revolution after the discovery. The results show that after three follow-

up observations during the same night the determined orbit has a sufficient accuracy for a successful recovery of a newly detected MEO object in the subsequent night.

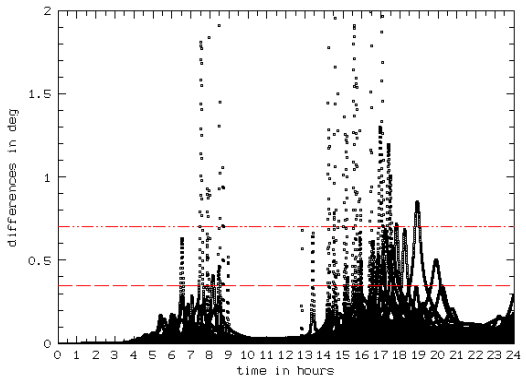

Figure 6: Difference Δ between "true" and elliptical orbit representing the discovery and all follow-up observations with a resulting arc length of 3 hours. Each curve represents the result from one of 100 simulated MEO orbits.

V. COVERAGE SIMULATIONS

Simulations have been performed with PROOF [RD 05]. The FoV, the exposure and gap time were chosen according to the ESA telescope characteristics.

A synthetic population within the following limits was simulated:

$$62\text{deg} < i < 67\text{deg}$$

$$0.5 < e < 0.75$$

$$23000\text{km} < a < 27000\text{km}$$

We set no limit for the nodes and for the argument of perigee and a homogenous distribution of the orbital elements was assumed. About 900 objects of this synthetic population were selected in a way to best represent the TLE population with similar distributions and relations between the orbital elements (POP1000). Every object was modelled as a sphere with a diameter of 1m and an albedo of 0.1.

Three similar observation strategies have been simulated over a time span of 90 days. A fixed declination of 55deg was chosen for all strategies. At first a single field in right ascension opposite to the sun was observed. In the second case a fence of three fields has been observed whereas the field in the middle of this fence was identical with that one from the first strategy. The two additional fields were displaced ±0.5deg in right ascension. Finally a fence consisting of four fields was simulated. The first field was identical with that one from the first strategy and all additional fields have been displaced +0.5deg in right ascension with respect to each other. The results show marginal differences in number of detected objects. One single object is observable during 20 nights before it leaves the field.

Because of the small FoV of the ESA TELESCOPE it is ambitious to cover the whole region. Therefore simulations over one year with ten nights of observation per month have been performed. A declination of 55deg was chosen again. The fields were displaced by 3deg in right ascension each night such that the field centres were always in anti-sun direction (see Figure 7). Each field was observed during one night. Finally more than 75% of the objects crossed the FoV and more than 70% of them could be detected under acceptable illumination conditions on at least one frame. Figure 8 shows the results of this simulation. All figures include a comparison of the crossings (black lines) and the detections (red lines). The FoV dwell time (Figure 8 top left) is less than 100 seconds for most of the objects. With an angular velocity of about 10arcsec/sec the maximum FoV dwell time is about 360sec. Most of the objects have an angular velocity of less than 50arcsec/sec (Figure 8 bottom, left) what corresponds to a maximum FoV dwell time of 72sec. The maximum phase angle is about 90deg (Figure 8 top, right) because of the observation geometry in anti-sun direction. Finally the magnitude of the objects is between 10mag and 17mag (Figure 8 bottom, right).

A variation of this scenario was simulated. Three observations per month were simulated. The same declination of 55deg was chosen but the fields were displaced by 10deg in right ascension each night. After one year about 25% of the POP1000 population cross the FoV and more than 60% of them could be detected on at least one frame.

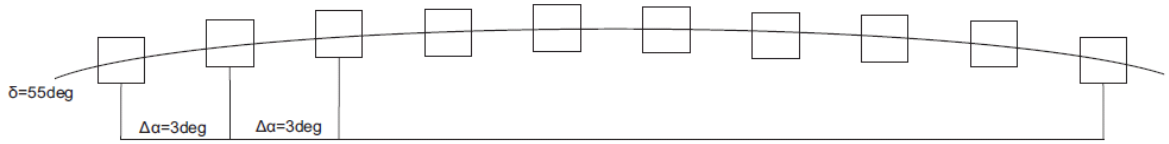

Figure 7: Survey strategy with 10 fields per month displaced by 3deg in right ascension

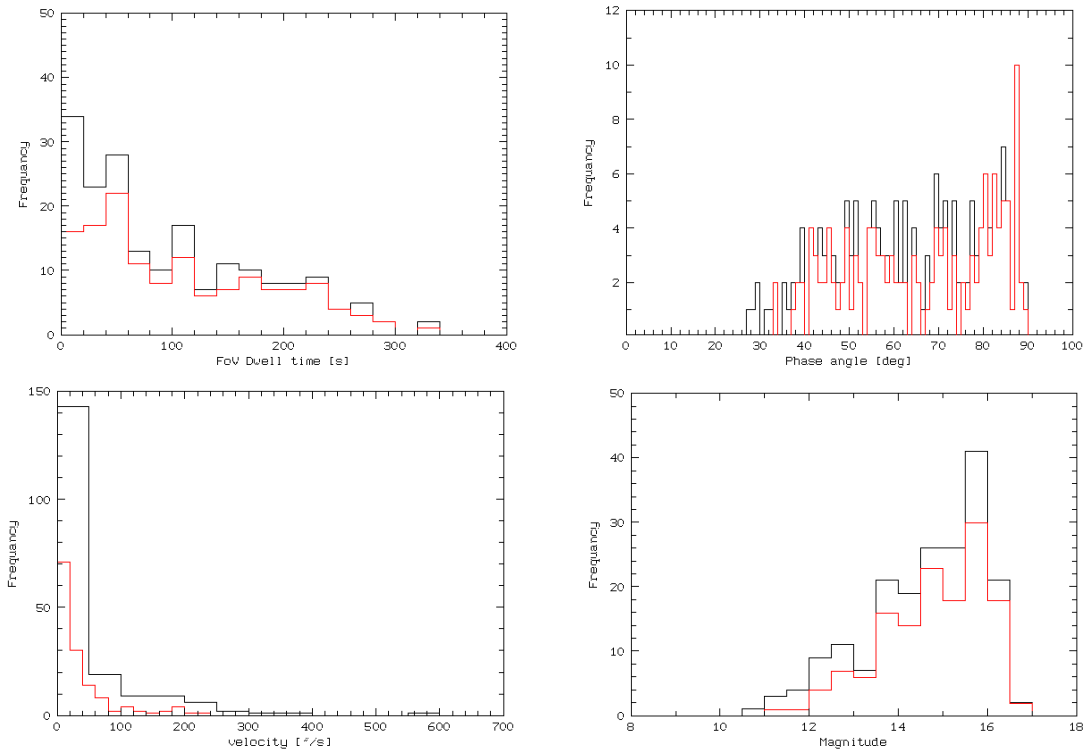

Figure 8: Results of the coverage simulation with POP1000 after one year with 10 nights/fields of observations per month. Crossings are given in black and detections are given in red.

VI. CONCLUSIONS

The MEO region is sparsely populated and the highest probability for detecting space debris is close to the orbital planes of known objects assuming that the orbital planes of most debris objects are similar to the ones of their parent objects. The evolution of the orbital elements shows that the distribution of the orbital elements of the current population is most likely very similar to the initial distribution.

A synthetic population of 100 eccentric MEO objects was used to simulate follow-up strategies. About three follow-up observations during the discovery night are necessary to determine an orbit with a sufficient accuracy for the successful recovery of a newly detected eccentric MEO object in the subsequent night.

Finally a synthetic population of 900 objects was used for coverage simulations. Using the ESA telescope, an entire scan of the region is ambitious due to its small FoV. Observing 10 nights each month for one year more than 50% of the population could be detected on at least one frame. This would allow a statistical analysis of the space debris population in the selected region.

VII. REFERENCES

[RD 01] T. Schildknecht, R. Murci, M. Ploner, et al., Optical observations of space debris in GEO and in highly-eccentric orbits. Adv. in Space Res., 34, 901-911, 2004

[RD 02] T. Schildknecht, R. Murci, M. Ploner, et al., Optical observations of space debris in high-altitude orbits, in: Danesy, D. (Ed.), Proceedings of the Fourth European Conference on Space Debris, ESA SP-587, ESA Puplications Division, Noordwijk, The Netherlands, pp. 113-118, 2005

[RD 03] T. Schildknecht, R. Murci, M. Serra Ricart, et al., Geostationary Transfer Orbit Survey. Final Report, ESA ESOC Contract 12568/97/D/IM, 2005.

[RD 04] G.Beutler. Methods of Celestial Mechanics. Two volumes. Springer-Verlag, Heidelberg, 2005

[RD 05] Program for Radar and Optical Observation Forecasting (PROOF), Final Report, ESOC Contract 18014/03/D/HK(SC), 2006

[RD 06] Hinze, T. Schildknecht, A. Vananti. Follow-up Strategies for MEO observations, In Proceedings of the 38th COSPAR Conference, 2010.